Nano Energy 45 (2018) 439–447

Contents lists available at ScienceDirect

Nano Energy

journal homepage: www.elsevier.com/locate/nanoen

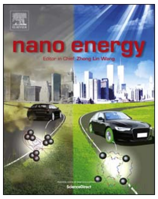

Full paper

# Hierarchically porous hexagonal microsheets constructed by well-interwoven $MCo_2S_4$ (M = Ni, Fe, Zn) nanotube networks via two-step anion-exchange for high-performance asymmetric supercapacitors

Juan Wu, Xiling Shi, Weijie Song, Hua Ren, Changbin Tan, Shaochun Tang*, Xiangkang Meng*

*National Laboratory of Solid State Microstructures, Collaborative Innovation Center of Advanced Microstructures, College of Engineering and Applied Sciences, Department of Materials Science & Engineering, Nanjing University, Jiangsu, PR China*

## ARTICLE INFO

*Keywords:*
Anion-exchange reaction
Ternary metal sulfides
Hierarchically porous structures
Nanotubes
Energy storage

## ABSTRACT

We report a significant advance in the design and fabrication of $MCo_2S_4$ (M = Ni, Fe, Zn) complex hierarchical structures with well-defined morphologies by achieving novel hierarchically porous hexagonal microsheets constructed by well-interwoven nanotube networks using a controllable two-step anion-exchange technique. Uniform and smooth hexagonal sheets are initially achieved for the first anion-exchange leading to nanowire-woven hexagons, followed by transformation of each nanowire to rough $MCo_2S_4$ nanotube via the second anion-exchange. The involved mechanism of this general top-down method allowing fine nanostructure control is clarified based on our proposed new insights into ion-induced anisotropic growth and time-dependent anion-exchange reaction kinetics. The merits of both maximized porosity and low resistance facilitate fast electron transfer/ion diffusion, thus $NiCo_2S_4$ electrode material exhibits a higher specific capacitance of 1780 F $g^{-1}$ and superior rate capability than most reported $NiCo_2S_4$ nanostructures with different morphologies as well as excellent stability (92.4% capacity retention after 10,000 cycles at 10 A $g^{-1}$). Furthermore, an asymmetric solid-state supercapacitor using such $NiCo_2S_4$ as positive and N-doped graphene film as negative electrodes achieves outstanding cycle ability (92.1% retention over 5000 cycles at 20 A $g^{-1}$) and higher energy density of 67.2 W h $kg^{-1}$ (at 900 W $kg^{-1}$) than that of similar devices. Such $MCo_2S_4$ electrode materials are promising for the future generation of high performance supercapacitors.

## 1. Introduction

Electrochemical capacitors (ECs) are extremely attractive as kind of efficient energy storage because of their fast charging capability, high service safety, and long life [1,2]. The relatively low energy density ($\leq$ 10 W h $kg^{-1}$) and unsatisfying long-term cycle stability at high charging rates are currently the main problems with ECs [3,4]. The key to address these issues is developing novel high-performance electrode materials [5–8]. Pseudocapacitive ternary transition metal sulfides such as $MCo_2S_4$ (M = Ni [9–13], Fe [14], Mn [15], and Zn [16,17]) are one kind of the most promising electrode materials. $MCo_2S_4$ exhibits much enhanced electrical conductivity than its oxide counterparts because a replacement of oxygen with sulfur creates a more flexible structure allowing easy electron transport, lower electronegativity and smaller band-gaps [18]. For example, $NiCo_2S_4$ has an electrical conductivity 100 times that of $NiCo_2O_4$, and four orders of magnitude higher than nickel or cobalt oxides [19–21]. Significantly, it exhibits higher electrochemical activity and capacity than single-metal sulfides based on the synergy from nickel and cobalt ions as well as multiple oxidation states facilitating richer faradaic redox reactions [22]. Usually, pseudocapacitive materials store charges only in the ~ 20 nm thick surface layer [23]. The other inaccessible volume is thus "dead" or "inactive" for electrochemical energy storage and results in a low utilization ratio of electrode materials [24]. To maximize utilization ratio of $MCo_2S_4$ structures with assuring both strong structure stability and high conductivity is still very challenging.

Nanostructures with a regular shape especially 1D nanowires (NWs) and nanotubes (NTs) exhibit superior electrochemical performance over irregular ones due to their high anisotropy and favorable orientations [25–27]. Bottom-up self-assembly of NWs/NTs can obtain porous assembles [26], but they are usually fragile and being unstable over time during rapid charge/discharge cycles; the contact resistance between adjacent individual NWs/NTs is typically too high to support fast electron transport [28]. Bottom-up grown hierarchical structures built by such 1D regular shapes are more likely to have better electrochemical performance because the architecture fixes the pores,

---

* Corresponding authors.
*E-mail addresses:* tangsc@nju.edu.cn (S. Tang), mengxk@nju.edu.cn (X. Meng).

https://doi.org/10.1016/j.nanoen.2018.01.024
Received 6 August 2017; Received in revised form 20 November 2017; Accepted 12 January 2018

isolates individual nanosized components from each other and stabilizes their distribution [29,30]. Particularly those with network architecture have low contact resistances and a large kinetically favorable exposed surface that can provide rich electro-active sites, electrode/electrolyte interfaces and short diffusion paths for redox reactions. Comparing with solid NWs, hollow NTs possess a larger effective active area by exposing both inner and outer walls [31,32]. For the synthesis of hollow structures, reported methods are usually based on a two-step process involving the first coating and subsequent removal of sacrificial templates [33]. Complex hierarchical NTs-architectures cannot be achieved yet by the traditional methods because of the deficiency of desirable complex templates and less controllable surface coating [34].

Ion-exchange reaction, called as self-template method [32], is an effective and low-cost method because it facilitates nanostructure control via a top-down route leading to complex hierarchical structures [11]. In particular, anion-exchange leads to hollowing of solid precursor wires/rods/spheres while keeping their overall morphologies and structures. $MCo_2S_4$ micro/nanostructures are generally synthesized in a solution by an exchange of the precursor anions and $S^{2-}$, during which composition transformation and structure modulation on the nanoscale can be achieved simultaneously. So far, the involved ion-exchange mechanisms for nanostructure modulation are still unclear and need further in-depth investigation. Great progress has been made in the controlled synthesis of $MCo_2S_4$ micro/nanostructures [11–13,35–37], however, using anion-exchange techniques in both the synthesis of complex hierarchical precursors and subsequent sulfidation for further fine nanostructure control has not been reported yet.

Herein, we report a significant advance in the design and fabrication of ECs' electrode materials based on a controllable two-step anion-exchange technique. Novel hierarchically porous hexagonal thin microsheets (HPHTMSs) constructed by well-interwoven $MCo_2S_4$ NT networks were achieved via this general top-down route. According to our new insights, NW-woven hexagons with central round holes were prepared by an ion-induced anisotropic growth and the first anion-exchange; the porosity is maximized combined with the second anion-exchange. The multiple channels in the HPHTMSs as ion transport shortcuts greatly accelerate ion diffusion across the entire volume, and NTs' wall thickness of < 20 nm allows their interior to be ion-accessible. Also, such NT-woven architecture has both a low contact resistance and strong structure stability. $NiCo_2S_4$ electrode shows a high capacitance of 1780 F $g^{-1}$ at 1 A $g^{-1}$, good rate capability, and excellent cycling stability (92.4% capacity retention after 10,000 cycles). Growth mechanisms and the reasons for performance enhancement were discussed in detail. An asymmetric solid-state device using the $NiCo_2S_4$ as positive electrode and porous N-doped graphene film as negative electrode achieves high cell voltage, energy densities and outstanding cycle ability, and its potential application as an electric source was further proved.

## 2. Results and discussion

The detailed preparation procedures are described in the Supporting information. Fig. 1 schematically illustrates the formation of HPHTMSs constructed by intersecting and well-interwoven $MCo_2S_4$ (taking $NiCo_2S_4$ as example) NTs through a controllable two-step anion-exchange process. Generation of $NiCo_2S_4$ NT-interwoven HPHTMSs is described as follows. At the beginning, the cations of $Co^{2+}$, $Ni^{2+}$, and $NH_4^+$ react with the anions of $CO_3^{2-}$ and $OH^-$ released from a slow hydrolysis of urea, which leads to $NiCo(OH)_x(CO_3)_y(HCO_3)_z$ regular hexagonal solid thin microsheets with smooth surfaces (defined as compound I). After 2 h reaction under the same environment, many well-dispersed tiny needles appear on edges and corners of each hexagon. 8 h later, these microsheets serving as matrix gradually convert to $NiCo_2(OH)_3(CO_3)_{1.5}$ hexagons with a NW-interwoven 3D porous architecture and a round central hole (defined as compound II) through an anion replacement of $HCO_3^-$ by $CO_3^{2-}$ and $OH^-$ ions. The possible chemical reactions are the following equations:

$$H_2NCONH_2 + 4H_2O \rightarrow CO_3^{2-} + 2NH_3{\cdot}H_2O + 2H^+ \tag{1}$$

$$NH_4F + H_2O \rightarrow NH_4^+ + F^- \tag{2}$$

$$NH_4^+ + H_2O \rightarrow NH_3{\cdot}H_2O + H^+ \tag{3}$$

$$CO_3^{2-} + H^+ \rightarrow HCO_3^- \tag{4}$$

$$Ni^{2+} + 2Co^{2+} + xOH^- + yCO_3^{2-} + zHCO_3^- \rightarrow NiCo_2(OH)_x(CO_3)_y(HCO_3)_z \tag{5}$$

$$NiCo_2(OH)_x(CO_3)_y(HCO_3)_z + (3\text{-}x+z)OH^- + (1.5\text{-}y\text{-}z)CO_3^{2-} \rightarrow NiCo_2(OH)_3(CO_3)_{1.5} + zH_2O \tag{6}$$

Interestingly, the generation of compound I and its morphology highly depend on the growth rate that is mainly determined by both the presence of $NH_4F$ and the mixed ions' concentration. Without $NH_4F$, compound I cannot be obtained as demonstrated by X-ray diffraction (XRD) analysis in Fig. S1a (Supporting information); the product is already compound II after only 0.5 h and its morphology is spherical with a rough NW-covering (Fig. S1b-c). In the presence of $NH_4F$, however, the generation of compound I needs about 1.5 h and obtaining pure compound II needs at the least 8 h. $F^-$ or $Cl^-$ ions are known to facilitate the anisotropic crystal growth, much similar to what was observed in the literature [38,39]. As for the concentration dependence, even if $NH_4F$ is used, large aggregations of compound I are the main products at high concentrations, e.g., with the typical doubled (Fig. S2a, Supporting information).

On one hand, to obtain the desirable nanostructure, a relatively slow reaction rate is necessary for anisotropic growth into single-crystalline compound I with a well-defined hexagonal morphology. On the other hand, a long enough reaction time is important for a complete composition conversion from surface to the interior. In the formation of compound I, $NH_4F$ lowers the nucleation and growth rate (Fig. S1). This could be attributed to the $NH_4^+$, as was further demonstrated by a control experiment where NaF was used instead of $NH_4F$ and the resulting product was already compound II after only 0.5 h, consistent with that without $NH_4F$. Also, $NH_4F$ slows the first ion-exchange reaction, in which the $NH_4^+$ provides $H^+$ (Eq. (3)) that combines with $CO_3^{2-}$ leading to the composition being $NiCo(OH)_x(CO_3)_y(HCO_3)_z$ (Eqs. (4) and (5)). Thus, the generation of compound I is mainly attributed to both $F^-$ and $NH_4^+$. Achieving compound I makes the subsequent ion-etching reaction along a top-down route to be possible. In the following conversion from compound I to compound II, $CO_3^{2-}$ and $OH^-$ from the hydrolysis of urea (Eq. (1)) participate in the first ion-exchange reaction, again the $NH_4^+$ in the solution plays a role of decreasing the reaction rate in this process. The slow hydrolysis of urea is also important for the morphology and nanostructure modulation [40]. Thus, this conversion process is mainly attributed to the $NH_4^+$ from ammonium salt, which is confirmed by the control experiments using $NH_4Cl$ instead of $NH_4F$ (Fig. S2b, Supporting information). To further demonstrate this, we carried out a control experiment by putting the pre-prepared compound I into a $NH_4F$ solution for another 5 h and 7 h (the total times are 6.5 h and 8.5 h) under the same hydrothermal environment as that for compound II. Surface etching due to the anion-exchange occurs because rough surfaces with many NWs are observed and NW-woven network appears again in Fig. S3b, Supporting information. Therefore, the $NH_4^+$ is decisive for the formation of compound II, because $NH_4^+$ played a vital role in both generation of compound I and subsequent conversion to compound II. The isotropic ion-exchange results in that compound II inherits the whole morphology of compound I. The nanostructure evolution with the reaction time is schematically illustrated in Fig. 1, and experimental demonstrations will be further discussed in detail later. By the second anion-exchange, the solid NWs in compound II were transformed to $NiCo_2S_4$ hollow NTs with a rough surface (defined as compound III). The insets illustrate local magnifications of